International Journal of Energy Research

INTERNATIONAL JOURNAL OF ENERGY RESEARCH
Int. J. Energy Res. 2014; **38**:1635–1653
Published online 13 April 2014 in Wiley Online Library (wileyonlinelibrary.com). DOI: 10.1002/er.3194

REVIEW PAPER

A review on carbon nanotube/polymer composites for organic solar cells

Godfrey Keru, Patrick G. Ndungu and Vincent O. Nyamori*,†

School of Chemistry and Physics, University of KwaZulu-Natal, Westville Campus, Private Bag X54001, Durban, 4000, South Africa

SUMMARY

Carbon nanotubes (CNTs) have unique properties, such as their electrical conductivity, that enable them to be combined with conducting polymers to form composites for use in organic solar cells (OSCs). It is envisaged that the improved composite has a higher efficiency of green energy and will reduce the cost of these cells. The use of such alternative energy sources also drastically reduces overuse of fossil fuels and consequently limits environmental degradation. This review compares research and performance between conventional silicon solar cells and OSCs. It also discusses OSC photoexcitation and charge carrier generation with the incorporation of CNTs, physicochemical properties of the composites and other factors that affect the efficiencies of OSCs. In addition, properties of CNTs that favour their dispersion in polymer matrices as acceptors and charge carriers to the electrodes are covered. The effects of CNTs containing dopants, such as nitrogen and boron, on charge transfer are discussed. Also, the fabrication techniques of OSCs that include CNT/polymer composite processing and the methods of film deposition on the substrate are described. Finally, the case studies of OSCs containing polymers with single-walled CNTs, double-walled CNTs or multi-walled CNTs are evaluated. Copyright © 2014 John Wiley & Sons, Ltd.

KEY WORDS

carbon nanotubes; conducting polymers; renewable green energy; CNT/polymer composites; organic solar cells

Correspondence

*Vincent O. Nyamori, School of Chemistry and Physics, University of KwaZulu-Natal, Westville Campus, Private Bag X54001, Durban, 4000, South Africa.
†E-mail: nyamori@ukzn.ac.za

Received 22 August 2013; Revised 28 February 2014; Accepted 28 February 2014

1. INTRODUCTION

Renewable energy accounts for approximately 16% of the primary energy sources used globally, while the rest is from less favourable options such as fossil fuels and nuclear power [1]. The primary factors in sourcing new and alternative sources of energy are ensuring positive and strong social economic development and the provision of abundant and reliable energy for domestic, industrial and various other economic sectors and also to harness enough energy to meet the demand of the growing population [2]. Globally, there is an intense interest and focus on the development of technologies that can use renewable sources of energy such as biomass [3,4], geothermal [5,6], solar [7], wind [8,9] and hydropower [10,11]. Some of the reasons for this can be attributed to the concerns surrounding energy security, the environment, sustainability, the drive for affordable energy services and the need to increase accessibility to economically viable energy options, especially where they lack in developing countries [2].

The usage of fossil fuels leads to environmental pollution through the release of greenhouse gases [12], and land degradation during exploration and mining. This in turn has been linked to acid rain, depletion of the ozone layer, harsh and sometimes unpredictable climatic conditions, the occurrence and spread of tropical diseases and other problems that adversely affect not only humans but also animals and plants. These appalling conditions can destroy fragile ecosystems, especially marine and aquatic life [2]. Despite these severe disadvantages of using fossil fuels, the implementation of renewable energy technology remains a challenge. This is mainly due to the intermittent nature of some renewable energy sources and geographically constricted environments (e.g. lower solar insolation at higher latitudes or impracticality of hydroelectric generation in arid and semi-arid regions). Moreover, in developing nations, heavy investments in infrastructure development are a challenge, and there are uncertainties and financial risk factors associated with renewable technologies [4,5,7].

Implementation and utilization of renewable energy technologies has several advantages including reliability and localization, diversification of energy supply, energy security, new wealth creation opportunities and a significantly smaller negative impact on the environment. In

addition, harnessing renewable energy at the local level will negate the vulnerabilities due to distant political upheavals, encountered in fossil fuel-producing regions. Furthermore, increased energy security through alternative greener sources would be advantageous, especially when supplies of various nonrenewable fuels dwindle and as demand increases. The 'norm' to circumvent this requires more costly explorations and potentially more dangerous extraction operations, which in turn increase the cost of energy. This makes investment in renewable energy technologies a better and more timely option.

Renewable technologies have zero emission of pollutants and utilize smaller amounts of water, thus destressing overburdened water resources. Moreover, they offer sustainable options for decentralization of energy supplies and thereby provide new opportunities in rural development and boost various agricultural activities [2,3]. Interestingly, most investments on renewable energy are on materials and workmanship to build and maintain facilities, rather than more energy input. This also means that because most of the resources are spent locally, there is a potentially huge foreign exchange savings that could be extremely beneficial especially in developing nations, which are often cash-strapped [13].

Amongst all of the various options available as renewable sources of energy, solar energy has some key advantages, especially when considering developing nations within Africa. Africa has some of the highest solar insolation-receiving regions on the planet because of its location in the tropics where incoming solar radiation mostly strikes the ground at an angle of 90° almost throughout the year [14]. Solar energy is free and clean; it does not produce waste, is ecologically acceptable and is directly convertible to other forms of energy. These advantages far outweigh the production of mild chemical waste that accompanies the manufacture of solar energy conversion technologies.

1.1. Solar energy

The earth receives 120,000 TW every hour from the sun and the estimated global energy requirement per year is approximately 13 TW [15]. Therefore, harnessing 0.01% of the energy the earth receives from the sun every hour will meet and surpass the annual global requirement and at the same time leave enough room for further growth and development to meet future needs. The technologies available for harnessing solar energy can be broadly categorized into two main areas. These are concentrating solar power [16] and solar photovoltaics (SPVs). In its simplest form, concentrating solar power focuses thermal energy from the sun into a heat transfer fluid by using mirrors. The heat generated is recovered to produce steam, which eventually is used to drive turbines and generate electricity. On the other hand, in SPV, electromagnetic energy is converted directly to electricity. Photons from the sun excite electrons in donor molecules, and these electrons are transferred to electrodes to generate electricity.

In developing countries, SPV technologies are one of the most attractive and elegant options available to provide energy. This is especially true for Africa, where the population is scattered over vast regions and where different groupings have divergent and dynamic electricity needs within various rural areas. In addition, the provision and maintenance of conventional electricity grids would be extremely challenging owing to environmental, economic, technical or a combination of some or all of these factors.

1.2. Inorganic versus organic solar cells

Currently, silicon-based cells have dominated commercial solar cell devices with approximately 90% of the global market share. Several factors account for this trend including both technical (e.g. silicon processing is a mature and reliable technology) and economic (widespread, commercially available technologies for silicon device manufacture) reasons. However, in terms of efficiencies, current research efforts have demonstrated that multijunction concentrator devices have overall efficiencies of over 30%, followed by crystalline silicon (~25%) [17], single-junction (~20.3%) [18], thin-film technology (~15%) [19] and eventually emerging photovoltaic (PV) devices, which include dye-sensitized and organic solar cells (OSCs) with efficiencies of less than 10% [13]. This is well illustrated in Figure 1, which shows efficiencies of different types of solar cells and their timelines on best research [13].

Silicon solar cells (SSCs), either crystalline (monocrystalline [20–22] and polycrystalline [23,24]) or amorphous [25,26], are generally expensive to manufacture and require a significant investment in labour and facilities. The main component, solar-grade silicon, is produced via several chemical steps, and a detailed description of the process is beyond the scope of this review. However, a brief and basic procedure involves the reduction of raw quartz with carbon to produce metallurgical silicon, which is relatively cheap to produce, but this is an energy-intensive process. The metallurgical silicon is then refined by converting the silicon to chlorosilanes (using HCl), and these are subsequently transformed, by using a chemical vapour deposition (CVD) process, into electronic or solar-grade silicon (i.e. the well-known Siemens process). There are other recent techniques that use plasma, or direct metallurgical processes, but these current technologies are energy intensive and can have detrimental effects on the environment [27–29]. These main drawbacks limit the implementation of silicon-based PV manufacturing within developing economies (many tropical countries, including South Africa). In the light of these challenges and circumstances, OSC technologies are favourable.

In general, OSCs can be described simply as PV devices made from polymers, small organic molecules or a combination of both with or without some kind of nanomaterial incorporated into the overall device. Mostly, these devices are based on polymeric materials and can thus be assembled by using well-known polymer-processing techniques. This

Int. J. Energy Res. 2014; **38**:1635–1653 © 2014 John Wiley & Sons, Ltd.
DOI: 10.1002/er

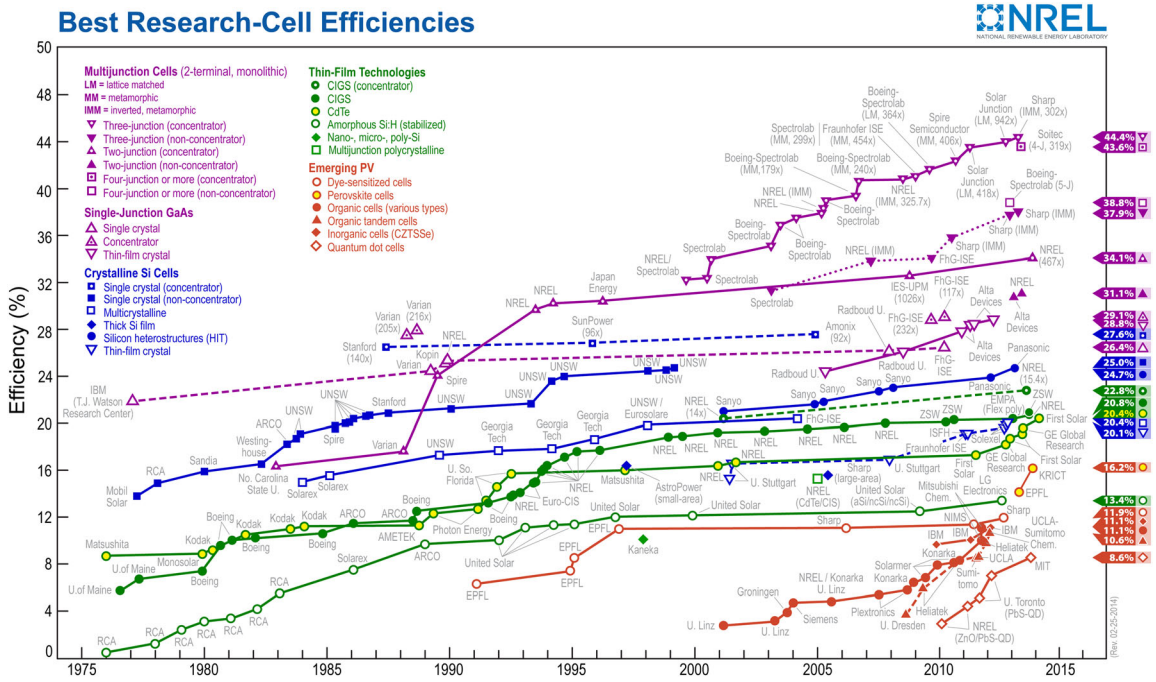

Figure 1. Timeline for best research and efficiencies for different solar cells reported so far [13].

means they are relatively simple to fabricate into various shapes and sizes (Figure 2) [30], are easily adapted and designed for niche applications, and can be assembled on various substrates and produced cost-effectively [31].

The basic architecture of an organic-based solar cell includes an active layer sandwiched between two transport layers that conduct holes or electrons and two electrodes that encase the whole structure, for harnessing the power generated. The active layer generates electron–hole pairs when excited by light, and at the interface between the transport layers and the active layer, the electron–hole pairs are separated, and these charge carriers are eventually collected by the electrodes and used to power the system of interest [32–36].

With silicon-based solar cells, separation of charge carriers occurs across a p–n junction, and this is enhanced by doping the material on either side of the junction. A similar scenario is encountered with other inorganic-based solar cells (e.g. CdTe, GaAs and CuInGaSe). With PV devices, ideally photon absorption excites an electron to the conduction band, which leads to the production of electron–hole pairs commonly known as excitons (electrostatically charged carriers). Excitons are characterized by a coulombic force (F) as shown in Equation 1 [37].

$$F = \frac{q_1 q_2}{4\pi r^2 \varepsilon\varepsilon_0} \quad (1)$$

where q is the charge, r is the distance between charges, ε is the dielectric constant and ε_0 is the permeability in the free state.

The theory and application in terms of physics and chemistry of inorganic systems are very well developed. In contrast, OSC's is still under intense investigation.

Figure 2. Organic solar cell cast on a flexible substrate. It can be stretched, rolled or even curved in any direction [30].

1.3. Photoexcitation and carrier generation in organic solar cells

With OSCs, the mechanism that leads to the separation of the electron–hole pair is a more complex process and is still an area under intensive investigation, but one of the key factors concerning their functionality is the heterojunction. The mechanism that leads to the generation of excitons, separation and final production of a useful photocurrent has been discussed recently in the literature [17,32,33]. The research findings reported so far indicate that photons, with the requisite energy, excite electrons within the donor molecule from the highest occupied molecular orbital (HOMO) to the lowest unoccupied molecular orbital (LUMO). This

produces excitons, polaron pairs, radical ion pairs or more generally a charge transfer complex, which can be envisaged to be analogous to the electron–hole pair in inorganic PV materials. The photoexcited charge transfer complex must then move (by either migration or diffusion) to the donor–acceptor (D–A) interface. The transfer of energy via charge transfer complexes may involve one or more transformations within the donor molecule, and similarly, there may be several energetic transition state complexes involving the donor, acceptor or combination of both at the D–A interface. The energy levels, HOMO and LUMO, within the donor are slightly higher than those of the acceptor. This is necessary to facilitate transfer of energy to the acceptor and reduce recombination within the donor. Thermal, radiative or electronic losses are possible near or at the D–A interface, but the generation of photocurrent occurs when the charge transfer complex separates into electron and hole charge carriers, with electrons in the acceptor material and holes in the donor, and eventually, they are collected at the electrodes [32,33,36].

1.3.1. Calculating efficiencies in organic solar cells

Photovoltaic properties for OSCs and SSCs are governed by the determination of the current–voltage of the cell; this is achieved by calculating either the power conversion efficiency (PCE) or the external quantum efficiency (EQE) of the cell. EQE is the ratio of collected charge carrier (electrons) per incident photon [38]. PCE of a cell is the efficiency of the cell under illumination of a standard light source or the percentage of solar energy exposed to a cell that is converted to electrical energy or electricity. A high PCE percentage translates to high output of that cell, and this can be improved by the development of new materials (e.g. conducting polymers with a low band gap) or device architecture [single junction, tendon cell and bulk heterojunction (BHJ)] [33]. Equation 2 shows how PCE is calculated.

$$\eta = \frac{V_{oc}\, I_{sc} FF}{P_{in}} \tag{2}$$

where V_{oc} is the open-circuit voltage, I_{sc} is the short-circuit current, P_{in} is the incident light power and FF is the fill factor. The fill factor measures the quality of the solar cell as a power source. It is the ratio between the maximum power delivered to an external circuit and the potential power of that cell and is determined as shown in Equation (3).

$$FF = \frac{V_{max} I_{max}}{V_{oc} I_{sc}} \tag{3}$$

where V_{max} is the maximum electromotive force in an electric circuit and I_{max} is the maximum rate of electron flow in an electric circuit.

A graphical relationship between V_{oc}, I_{sc}, V_{max} and I_{max} is shown in Figure 3.

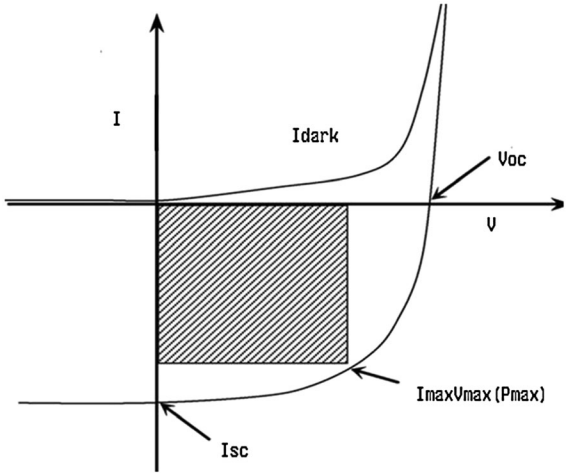

Figure 3. Relationship between V_{oc}, I_{sc}, I_{max} and V_{max} in the dark and under illumination. The shaded area is used to determine V_{max} and I_{max} [39].

1.3.2. Physicochemical factors that affect the efficiency of organic solar cells

Organic solar cells have low PCE and are short-lived when compared with SSCs, and this limits their practical application [31]. The short lifetime is due to chemical and physical degradation of the active layers and electrodes. Chemical degradation involves chemical changes within the organic materials or on the electrodes due to the presence of oxygen and moisture (Figure 4) [40]. Physical degradation is usually caused by charge accumulation, morphological changes or diffusion of metal into the active layer [31]. Electrodes degrade by oxidation, delaminating, dedoping and interfacial organometallic chemistry. Active layers degrade via photochemical reactions, thermochemical reactions, morphological changes

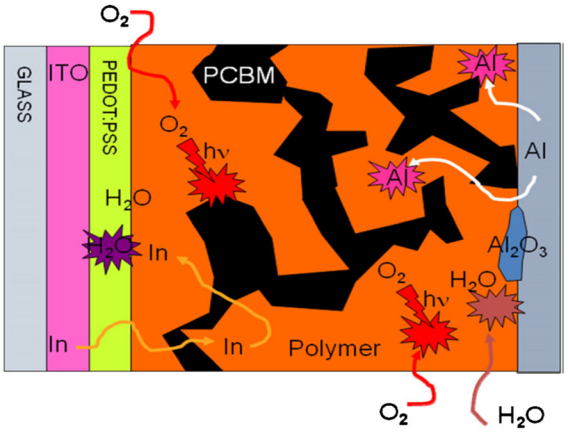

Figure 4. Degradation of the active layer due to the presence of oxygen and water, as well as diffusion of metal electrode particles into the active layer. Oxygen and water enter the device during the fabrication process [40].

Int. J. Energy Res. 2014; **38**:1635–1653 © 2014 John Wiley & Sons, Ltd.
DOI: 10.1002/er

and inclusion of impurities [41]. Degradation can also occur because of low photostability of the active layer–electrode interface, and this can be minimized by depositing a thin film of electron extraction layer and hole extraction layer between the active layer and the electrodes [42]. It has been reported that an active layer with chemically active side groups is more susceptible to degradation than one without. Jorgensen *et al.* [34] were able to show that degradation due to oxidation usually occurs at the side groups. Low PCE with OSCs can also be due to efficiency loss that occurs in the first few hours of exposure to the atmosphere known as burn-in [41]. This crucial loss in functionality can be ascribed to photochemical reactions in the active layer and the development of trap states within the band gap [41]. Performance also reduces because of other mechanisms, which include trap-mediated recombinations, reduced hole mobility and build-up of charge in various trap states.

One of the main limiting factors in achieving high PCE in OSCs is the recombination mechanisms that occur at the D–A interface. Some of the methods developed to minimize recombination include improving device morphology [43], using modified D–A materials [44], manipulating electrode materials [45] and even enhancing optical absorption [46]. Zhang *et al.* [47] have reported a significant reduction in recombination losses by doping the active layer poly(3-hexylthiophene) (P3HT)/(6,6)-phenyl-C_{61}-butyric-acid methyl ester (PCBM) with 1/2 spin galvinoxyl radicals at the D–A interface, which increases the PCE of the device by ~340%.

Another factor that affects the efficiencies of OSCs is the band gap of the conjugated polymers. When the band gap of the semiconducting conjugated polymer is large, only a small portion of the incident solar energy is absorbed. For example, a polymer with a band gap of ~2.0 eV can only absorb 25% of the solar energy. Reduction of the band gap to ~1.2 eV enhances absorption to between 70% and 80% [48] as shown in Figure 5. For maximum absorption,

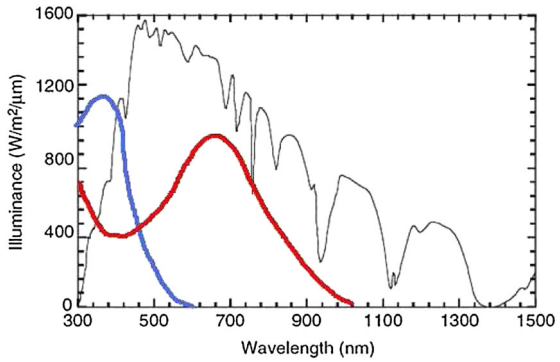

Figure 5. The solar spectrum together with the absorption spectra of two polymers showing the limitation of absorption due to the band gap size. The blue line shows the absorption of a polymer with a band gap of ~2 eV and the red of ~1.2 eV. The black line represent AM 1.5 illumination [48].

a smaller band gap is favourable. Of interest is to make use of low-energy-band-gap materials with a value of band gap energy (E_g) of 1.5 eV or less so that absorption will occur at 600 nm or greater in the neutral state [38].

Efficiencies of OSCs can be improved by incorporation of carbon nanotubes (CNTs) in the BHJ. For example, Somani and co-workers reported improvement of cell performance by many fold by incorporation of double-walled CNTs (DWCNTs) to P3HT [49]. CNTs can be a good material at the interface because they have a high affinity for electrons and also transport electrons to the electrodes unlike fullerenes, which are only good electron acceptors [50]. CNTs have also found use as transparent electrodes for hole collection owing to their high work function, replacing indium tin oxide (ITO). However, this is a topic of another review, and we recommend the reader to references [51–55]. Arena and co-workers reported that efficiency conversion of hybrid cells based on a conjugated polymer and doped silicon increased by 0.49% upon dispersion of CNTs in the conjugated polymer layer [56]. Efficiencies of OSCs can be enhanced further by using CNTs with heteroatom dopants such as boron or nitrogen. Doping of CNTs with nitrogen or boron to form N-CNTs or B-CNTs introduces defects that change the structural, chemical and electronic properties [57]. Lee and co-workers reported a high efficiency of 5.29% by incorporating N-CNTs in OSCs. The cell had an efficiency of 4.68% before incorporation of N-CNTs [58].

2. INCORPORATION OF CARBON NANOTUBES IN ORGANIC SOLAR CELLS

Inclusion of conducting nanostructures like CNTs in the BHJ enhances charge separation and improves transfer of charge carriers to the electrodes before they recombine. CNTs can combine with the π-electrons of conjugated polymers to form D–A-type solar cells [59]. Here, the CNTs do not only act as electron acceptors but also improve the dissociation of excitons by providing an enhanced electric field at the CNT/polymer interface, which suppresses the recombination of photogenerated charges. CNTs in the BHJ of a polymer matrix result in high electron mobility, which exceeds that of any other semiconductor [60]. Likewise, hole transport is also enhanced because of induced crystallinity of poly(3-octylthiophene) (P3OT) or other conducting polymers. Highly ordered supramolecular organization of the conducting polymer ensures higher hole mobility via interchain transport [60].

Carbon nanotubes are dispersed in a solution of donor polymer before being spin-coated on the substrate. The substrate is usually a transparent electrode consisting of a transparent conductive oxide of which ITO is an example [30]. Firstly, a hole conducting layer of poly(3,4-ethylenedioxylthiophine) : poly(styrenesulfonate) is deposited, which helps in selective hole injection to the ITO

electrode as illustrated in Figure 6. An active layer consisting of the donor–acceptor is then deposited. Conjugated polymers, like P3HT or P3OT, are used as the donor components because of their ability to form semicrystalline films when cast on a substrate [39], while fullerenes or CNTs can be the acceptor. Thermal annealing at a temperature above the polymer glass transition temperature allows the alignment of the polymer chains, thereby improving charge transfer. The top electrode is vacuum evaporated and is usually a metal of lower work function (as compared with ITO), such as calcium or aluminium, and sometimes with an ultrathin lithium fluoride underlayer [61].

Sometimes, a third component like a dye is incorporated into the active layer to improve the PV properties of a cell. Bhattacharyya *et al.* [62] used the dye *N*-(1-pyrenyl) maleimide (PM) in the single-walled CNT (SWCNT)/P3OT composite to form a cell ITO/P3OT-SWNCTs + PM/Al that improved the cell efficiency by two orders of magnitude. The group attributed this increase to efficient charge carrier transfer as illustrated in Figure 7.

Doping CNTs with boron or nitrogen selectively enhances charge mobility and dispersibility in the polymer matrix and also tunes the work function [63]. For effective charge transfer, the work function of the CNTs should be close to the HOMO and LUMO of the donor and receiver, respectively [64]. B doping reduces the Fermi-level energy of the CNTs and at the same time increases the work function [65]. Upon B doping, the work function increases to 5.2 eV from 4.6 eV of pristine CNTs, which is very close to the HOMO of the P3HT (5.1 eV) donor [64]. This makes it very easy to inject a hole to the B-CNT for eventual transfer to the electrode. However, doping CNTs with electron-rich nitrogen increases the Fermi-level energy and reduces the work function in comparison with pristine CNTs [63]. For N-CNTs, the work function is 4.4 eV, which is very close

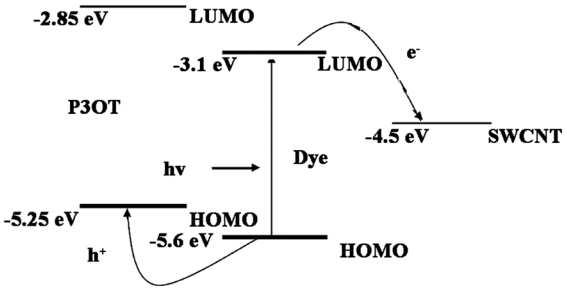

Figure 7. Movement of charge carriers between the energy levels of the donor polymer (P3OT) and dye with the eventual transfer of an electron to the SWCNT. Because the work function of the SWCNT is slightly lower than the LUMO of the dye, the transfer of an electron is easy [62].

to the LUMO of the receiver PCBM (4.2 eV) in OSCs. An electron can easily move from the LUMO of PCBM to N-CNTs because of the short distance between the LUMO of PCBM and the work function of N-CNTs (~0.2 eV), electrons are then to be transferred to the electrode. At the same time, use of either B-doped or N-doped CNTs in the BHJ of a polymer matrix makes charge recombination almost impossible. Mismatch of energies between the HOMO of the donor and N-CNTs and the LUMO of the receiver and B-CNTs makes it hard for dissociated charges to recombine as the hole is received by B-CNTs and electrons by N-CNTs [58]. B-doped or N-doped CNTs improve the I_{sc} and PCE of a cell and also help in the alignment of CNTs in the polymer matrix because of local polarities induced on the walls of CNTs and because the defects caused by the heteroatoms converts them from nonconducting to conducting materials [39,65].

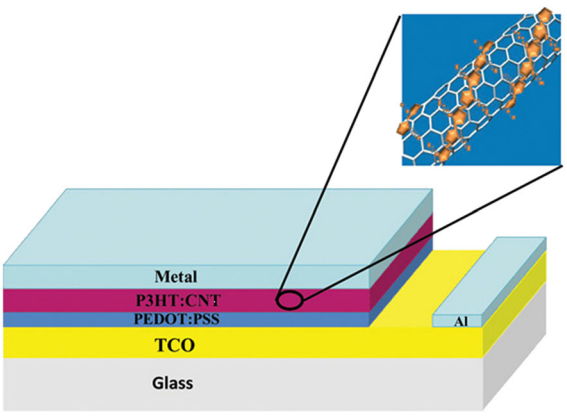

Figure 6. A schematic diagram showing the sandwiched active layer between the electrodes in OSCs with CNTs as acceptors within the active layer. Inset: high magnification of the active layer showing how polymer wraps onto CNTs [30].

2.1. Advantageous properties of carbon nanotubes for organic solar cells

Carbon nanotubes are synthesized in a number of different ways depending on the resources available and research objective. However, most methods are a variation on either the arc discharge [39], laser ablation [66] or CVD method [67–69]. The CVD method is the most preferred technique because it is easy to implement and scale up [70,71]. The synthesis technique has a direct impact on the final properties of the CNTs. The arc discharge and laser ablation techniques favour SWCNTs or highly graphitic multi-walled CNTs (MWCNTs). CVD methods usually produce MWCNTs; however, SWCNTs and DWCNTs can be grown.

When CNTs are incorporated into a polymer matrix, the resulting nanocomposites have significantly different physical–chemical properties than the original polymer material. The importance of the physical–chemical properties of CNTs

Int. J. Energy Res. 2014; **38**:1635–1653 © 2014 John Wiley & Sons, Ltd.
DOI: 10.1002/er

in the polymer matrix and the significance of incorporating CNTs in OSCs are discussed in the next section.

2.2. Physicochemical properties of carbon nanotubes

Carbon nanotubes are good conductors of electricity, and their conductivity is 1000 times that of copper [70], and thus, when incorporated into a polymer matrix such as that for OSCs, they can provide an excellent and robust network for the transfer of charge carriers to the electrodes by providing a percolating path [72]. Semiconducting CNTs also generate excitons upon absorption in the near-infrared region of the electromagnetic spectrum [73]. This has the potential to increase the number of excitons generated within a device and results in a greater number of disintegrations to electrons and holes when incorporated into OSCs. CNTs have a high aspect ratio (>1000:1), and therefore, very little is required to form composites with physicochemical properties that are very different from those of the parent polymer [73]. They have outstanding mechanical properties [74], a high surface area-to-volume ratio [75] and relatively small diameters, which have made these materials very useful as additives to make high-strength composites [76].

2.2.1. Electronic properties of carbon nanotubes

Single-walled CNTs can have either metallic or semiconducting properties depending on the orientation of the graphene sheets, which are rolled to make the individual tube [77]. In a perfectly aligned SWCNT, there is overlap of π-orbitals in the individual six-membered rings. This overlap provides a delocalized space for the movement of electrons, and the SWCNTs are deemed conductors. The conductivity can change to semiconducting when the alignment of the six-membered rings is distorted, and thus, the π-orbital overlap is changed. The direction of the graphene sheet plane and the nanotube diameter are obtained from a pair of integers (n, m) that denote the nanotube type [78]. In the *armchair* configuration, the integers are equal ($n = m$), and in the *zigzag* orientation, one of the integers is equal to 0 (m or $n = 0$), and when the tube is described as *chiral*, the integers are nonzero and nonequal ($n \neq m$). Armchair-type tubes are metallic, while all other orientations are semiconducting [79]. At high temperatures, the electrical conductivity of SWCNTs can be described by using semiclassical models used with graphite, while at low temperature, they reveal 2D quantum transport features [80]. However, it is very difficult to predict the electrical properties of MWCNTs because rolling up of the graphene layers can differ from one layer to the other and their more complex structure increases the possibility of defects, which can alter the electronic properties.

In terms of electrical properties, some recent reviews have highlighted the limitations encountered when incorporating SWCNT structures into OSCs [81–84]. Nevertheless, the key consideration is the inhomogeneity of a sample of SWCNTs. Typically, after synthesizing and purifying SWCNTs, the samples contain a mixture of semiconducting and highly conducting tubes. Thus, some of the tubes may enhance charge carrier transfer to the electrodes, and some may act as sites for recombination of charge carriers. These limitations may be overcome in the near future, with improvements in the synthesis of SWCNTs to control chirality or in separation methods.

When CNTs, multi-walled or single walled, are incorporated into a polymer matrix, the resulting nanocomposites can have electrical properties that differ from their parent materials. This depends on whether the loading or weight per cent of CNTs is above or below the percolation threshold. Conductivity increases drastically when the amount of CNTs is at or above the percolation threshold. Bauhofer and Kovacs have reviewed percolation thresholds for CNT/polymer composites [85]. The percolation threshold is known to be influenced by dispersion, aspect ratio, purity and alignment of the CNTs [86]. Also, it has been suggested that it is easier for well-dispersed CNTs to form an electrical path owing to homogeneous dispersion [85]. Higher electrical conductivity leads to increased photocurrents, which improve the overall efficiency of the cell device [87].

The electrical properties of SWCNTs and MWCNTs can be tuned to a certain extent, whereby the HOMO and LUMO match the donor and acceptor polymers appropriately, and thus, these materials can be incorporated into the OSC architecture as electron or hole carriers within the donor or acceptor polymer matrix or as transparent electrodes [88].

2.2.2. Mechanical properties of carbon nanotubes

Carbon nanotubes are made of sp^2 carbon–carbon bonds, and these continuous networks within a tubular shape make them some of the strongest and most resilient materials known to exist. CNTs have a theoretical Young modulus on the scale of terapascals, and the tensile strength of these materials has been measured to be upwards of 100s of gigapascals. To offer some perspective on such numbers, CNTs are often compared with steel, with simple descriptors stating they are 100 times stronger than steel but weigh six times less [78,89–91]. In addition, CNTs are also very flexible and can bend over 90° several times without breaking [92]. They undergo permanent structural changes at high pressures (>1.5 GPa), but below these values, deformation is usually totally elastic [80]. Also in the radial direction, CNTs have a much lower Young modulus of 10s of gigapascals, and the tensile strength in the radial direction is lower with values of ~1 GPa. The mechanical strength of CNTs increases the strength of the CNT/polymer composite [78,89–91,93,94] and can be of interest to OSCs [72]. The transfer of the mechanical properties of the CNTs to the polymer matrix or the change in mechanical properties from

those of the parent materials to the new composite offers new possibilities in the design and implementation of solar cells in general. The use of lighter and stronger materials means that larger-surface-area PV systems can be assembled on structures that cannot support the weight of some inorganic systems. In addition, the flexibility would allow for greater options in design and implementation, for example, OSCs on a bridge column or any other highly curved surface. However, in order to achieve excellent mechanical properties with polymer/CNT nanocomposites, the CNTs need to be functionalized in order to debundle them and to facilitate dispersion in a solution or polymer matrix.

2.2.3. Thermal properties of carbon nanotubes

Among the carbonaceous materials, CNTs are more stable to oxidation than activated carbon or amorphous carbon at high temperature. The thermal behaviour is different in SWCNTs and MWCNTs. SWCNTs are more thermally stable than MWCNTs because they have more defined structure and less deformations [90]. The thermoconductivity of CNTs in the axial direction is higher, while in the radial direction, it is an insulator. The estimated thermoconductivity at room temperature is $7000\,W\,m^{-1}\,K^{-1}$ [95]. This is comparable with that of diamond; therefore, inclusion of CNTs in the polymer matrix forms a thermally conductive percolating network enhancing thermal conductivity [96]. For OSCs, this can improve thermal conductivity, and hence, it may reduce thermal degradation problems.

2.2.4. Chemical properties of carbon nanotubes

Generally, CNTs are chemically inert, but the curvature on the surface of the tubes enhances their reactivity compared with a flat graphene sheet [97]. Mismatch between the π-orbitals in the CNT walls brings about reactivity enhancements. CNTs with small diameters are more reactive than ones with bigger diameters [97]. The slight reactivity of CNTs allows surface modification, and this is accomplished by acid oxidation to introduce oxygen-containing group functionalities on the wall surfaces [98], which increases solubility in polar solvents and also increases their compatibility with some polymeric matrices [93]. Further modification is possible through covalent chemistry and examples include fluorination, ozonolysis or acrylation [78]. These modifications of CNTs are known as functionalization and are discussed in the next section.

2.3. Functionalization of carbon nanotubes

Raw CNTs are not usually used to make CNT/polymer composites without treatment to eliminate impurities like amorphous carbon, metal particles and graphitic nanoparticles, all of which interfere with the desired properties or end product [99]. These impurities can be removed by gas-phase oxidation [100], acid treatment [101], annealing and thermal treatment [102,103], ultrasonication [99], magnetic separation [99], microfiltration [102] or a combination of two or more of the aforementioned methods [104].

As previously mentioned, incorporation of CNTs in a conjugated polymer has potential use in OSC fabrication as it improves the mechanical, thermal and electrical properties of the polymer [62]. However, for improved interfacial bonding and good dispersion of the CNTs in a conjugated polymer or solvent, surface modification is required. Surface modification can either be covalent or noncovalent [105]. Table I shows how these two types of functionalization are achieved.

2.3.1. Noncovalent functionalization

Noncovalent modification involves physical adsorption of the polymer chain on the walls of the CNTs through interaction of the delocalized π-electronic structure of CNTs and the delocalized π-electronic structure of conjugated polymer chains [109]. Interaction between the π-electronic systems of the polymer chains and the CNT walls breaks the van der Waals forces between individual CNTs. Typically, CNTs aggregate

Table I. Surface functionalization of carbon nanotubes.

Type of functionalization	Method of functionalization	Reagents	Damaging effect on carbon nanotubes	References
Noncovalent	Sonication followed by *in situ* polymerization	Dianhydride monomer	Yes	[106]
	Surfactant-aided modification	Sodium dodecyl sulfonate	No	[107,108]
	Wrapping	Polyvinylpyrrolidone	No	[109]
Covalent	Solution treatment (usually acid oxidation)	Concentrated H_2SO_4 : HNO_3 (3:1)	Yes	[110,111]
	Ball milling	Gases, for example, H_2S, NH_3, CO and $COCl_2$	Yes	[112,113]
	Plasma treatment	N_2/Ar microwave plasma treatment to introduce N_2 on the wall	No	[114]

into bundles owing to the dispersion forces between individual tubes, and the high aspect ratio means the bundles can be very difficult to break up, hence the use of ultrasound probe techniques during processing. The interaction between the polymer chain and individual CNTs modifies the conformation of the polymer and can lead to helical wrapping around the CNT. Noncovalent functionalization does not interfere with the conjugated system of the CNTs, and therefore, the desired properties are retained [115].

2.3.2. Covalent functionalization

Covalent functionalization or a chemical modification introduces functional groups covalently bonded to the backbone structure of the CNTs and contributes to better dispersion of CNTs within the polymer matrix. It also improves the chemical affinity of CNTs, which assists in the processing of the CNT/polymer composite and improves the mechanical and electrical properties of the composite [115]. However, covalent functionalization can alter the electronic properties of CNTs in an unfavourable manner, and this can have an unfavourable effect on the final OSCs.

3. ASSEMBLING SOLAR CELLS

The production of OSCs with CNTs involves a number of steps including processing of the conjugated polymer/CNT composites and deposition of these composites onto a suitable substrate.

3.1. Processing conjugated polymer/carbon nanotube composites

Good dispersion and adhesion of the CNTs with the polymer matrix play an important role in incorporating the excellent properties of CNTs in the polymer matrix [86]. There are several methods of processing CNT/polymer composites, which include solution mixing, melt blending and *in situ* polymerization. Effective utilization of CNTs in composite applications depends on their ability to disperse individually and homogenously within the polymer matrix. Interfacial interaction between the CNTs and the polymer matrix results in efficient load transfer. It also affects the alignment of individual tubes in the polymer matrix [115]. Well-aligned tubes are reported to interact well with the polymer matrix, which enhances conductivity and increases the mechanical strength of the composite [116].

3.1.1. Solution processing

The general procedure involves dispersion of CNTs in a suitable solvent by energetic agitation, followed by mixing of polymer and nanotubes in solution by mechanical agitation. The solvent is then allowed to evaporate under controlled conditions, and the CNT/polymer composite is left behind [86]. Energetic agitation can be brought about by shear intensive mechanical stirring, magnetic stirring or ultrasonication [115].

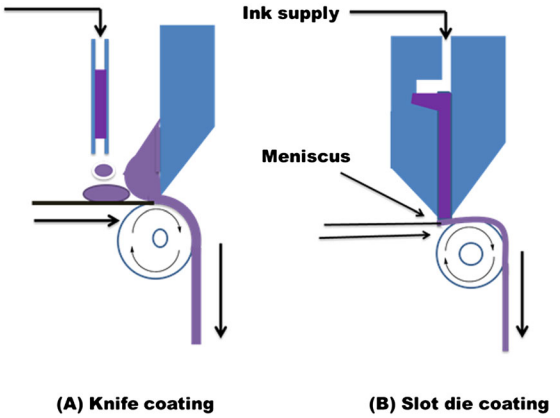

Figure 8. Illustration of knife coating (A) and slot-die coating (B). The coat is deposited on the web as it passes [127].

Prolonged use of high-powered ultrasonication can introduce defects on the nanotube walls and reduce their sizes, which affects their properties [86]. Bhattacharyya *et al*. [62] processed a P3OT/SWCNT composite by solution processing. The CNTs were dispersed in chloroform by high-powered ultrasonication, the P3OT solution in chloroform was added to this dispersion and the mixture was then sonicated. The chloroform solution was left to evaporate. Geng and Zeng similarly prepared a composite P3HT with SWCNTs by solution processing [117].

Nogueira and co-workers prepared a composite of SWCNTs and thiophene by using solution processing [118]. However, in their case, they first dried the oxidized SWCNTs and then followed by refluxing them with 3 M nitric acid to introduce carboxylic acid groups. Thionyl chloride was then added, and the mixture was stirred to introduce acyl chloride groups. Thereafter, 2(2-thienyl)ethanol was added to form an ester named SWCNT-THIOP. The product was dispersed in toluene, the polymer P3OT was added, the mixture was stirred and the toluene evaporated, leaving the composite that they characterized.

3.1.2. Melt processing

This method involves heating the polymer above its melting point to form a viscous liquid and introducing the CNTs by shear mixing. The method is good for insoluble polymers that are impossible to prepare by solution processing. It is the most compatible method with current industrial practices such as injection moulding, blow moulding, extrusion and internal mixing. In particular, this technique is very useful when dealing with thermoplastic polymers, which soften when heated [119]. Socher *et al*. [120] used melt mixing to incorporate MWCNTs and carbon black together as fillers in polyamide 12. The aim was to study the synergistic interaction effect of the two conductivity fillers. They reported higher volume conductivities for samples with the two fillers together although no synergistic effect was reported at the percolation threshold.

3.1.3. *In situ* processing

The method involves dispersion of CNTs in a monomer solution. Polymerization takes place to form the polymer/CNT composite and is usually good for polymers that are not soluble or are thermally unstable. *In situ* polymerization can prepare composites that are covalently or noncovalently bound to the nanotubes [86]. Because of the small size of monomer molecules, the homogeneity of the resulting composite adducts is much higher than solution mixing of polymer and CNTs. It also allows preparation of composites with a high CNT weight fraction [115]. The advantage of this method is the high reactivity of monomers that makes it efficient and controllable and enables designable tailored processing.

Koizhaiganova *et al*. [121] synthesized a P3HT/DWCNT composite by *in situ* polymerization to enable interfacial bonding and proper dispersion of the CNTs in the polymer matrix. They reported impressive conductivity values and recommended the use of the composite as a PV cell material. The same group had earlier reported the synthesis of a P3OT/DWCNT composite by *in situ* polymerization [121] and reported that the inner walls of the DWCNTs retained their intrinsic properties, while the outer walls were involved in the formation of the composite with the polymer. This explains why composites are popular in solar cells. Kim *et al*. [122] synthesized MWCNT/P3HT composites by *in situ* polymerization. They reported that the MWCNTs provide good conductivity even at low loading. Impressive conductivities and mobility values of the composite make it suitable for use in PV materials.

3.2. Film deposition techniques

Carbon nanotube/polymer composite processing is followed by deposition or coating onto a suitable substrate in order to fabricate OSCs. Deposition techniques involve depositing a thin film of material on a substrate or previously deposited layers. The key issue is to have control on the layer thickness to a few tens of nanometres. The following are some of the methods used to deposit the organic films on the substrates.

3.2.1. Spin coating method

This involves dosing CNT/polymer composite on the substrate that rotates, distributing the composite homogeneously on the surface owing to centrifugal forces. The substrate spins until the composite dries up, and the final thickness is controlled by the frequency of the spin, composition and properties of the material as well as the drying conditions. Spin-coating parameters are interdependent on each other; for example, an increase in spin frequency results in a lower film thickness, higher drying rate and higher shear rate [123]. Nagata *et al*. [124] used spin coating to prepare a BHJ OSC with coplanar interdigitized electrodes. Vairavan and co-workers used spin coating to deposit the active layer of poly[2-methoxy-5-(2-et hylhexyloxy)-1,4-phenylenevinylene], CdTe and CdS hybrid on a substrate, and the PCE of the device increased by 0.05% [125]. Singh *et al*. [126] used spin coating of P3HT, functionalized SWCNTs and PCBM composite on a substrate at ambient conditions and formed a cell with a photoefficiency of ~1.8%.

3.2.2. Knife coating and slot-die coating method

These techniques involve continuous deposition of a wet layer along the length of the web without contact with the coating head and the web. Coating is a result of feeding the CNT/polymer composite suspension to a meniscus that stands between the coating head and the web (Figure 8). Coat thickness control is superior to printing. Knife coating is very similar to doctor blading, and laboratory results show that it can be transferred quite readily to roll-to-roll knife coating [127]. An ink reservoir before the knife in the knife coating process serves as a supply to the meniscus with new ink; as the web passes by, it gradually deposits.

In the case of slot-die coating, the suspension is supplied to the meniscus via a slot and a pump. With this method, it is also possible to coat stripes of a well-defined width along the web direction, and hence, it is one of the only film-forming techniques that inherently allows for 1D patterning. This aspect has enabled the very convincing demonstration of slot-die coating for the manufacture of polymer solar cells. It is possible to control and adjust the coat layer by controlling the speed of the web or the CNT/polymer suspension supply. Wengeler and co-workers investigated knife and slot-die coating to process a polymer nanoparticle composite for hybrid polymer solar cells [123]. They reported that knife-coated solar cells showed efficiencies comparable with those of spin coating, which demonstrates scalability because knife coating is compatible with the roll-to-roll technique.

3.2.3. Inject printing and spray-coating method

With these types of wet-film techniques, a coat is formed without contact between the substrate and the printing head. CNT/polymer composite suspension droplets are ejected into the free space that exists between the nozzle and substrate. The coat thickness can be controlled by printing multiple layers or adding more composite suspension to one spot [127]. Girotto *et al*. [128] used both spray and spin coating to compare composite performance. They demonstrated that spray coating is an excellent alternative to spin coating. Peh *et al*. [129] reported spray coating as a high-throughput coating technique that is scalable and adaptable for organic photovoltaic manufacturing. They argued that, to ensure uniform coating of the organic layer, the wettability, surface tension and boiling point of the solvent require optimization. Kang and co-workers used a spray-coating process to deposit electron-selective and hole-selective layers in an inverted OSC [130].

3.2.4. Dip coating technique

Materials used for dip coating are dissolved in an appropriate solvent such as toluene, chloromethane or chlorobenzene [131]. The substrate is soaked upright by allowing full coverage by the solution. Then the substrate

Int. J. Energy Res. 2014; **38**:1635–1653 © 2014 John Wiley & Sons, Ltd.
DOI: 10.1002/er

Table II. Examples of CNT/polymer composites in organic solar cells.

Type of CNT used	CNT treatment/ functionalization	CNT loading (wt%)	Polymer used	CNT dopant	Additional composite additives	Position within the device	V_{oc} (mV)	J_{sc} (mA cm^{-2})	*FF*	η %)	Illumination	Reference
MWCNT	Oxidation (mix of H_2SO_4 and HNO_3)	2.00	P3HT	N/A	Graphene	Active layer	670.00	4.7000	0.320	1.050	100 mW cm^{-2}	[38]
MWCNT	Alkyl amide side chains (octyldecylamine)	0.20	P3HT	N/A	PCBM	Active layer	560.00	14.7900	0.520	4.390	AM 1.5 G, 95 mW cm^{-2}	[87]
SWCNT	Carboxylated and sulfonated	0.40	P3HT	N/A	C60	Active layer	386.00	2.7200	0.512	0.570	AM 1.5 G, 95 mW cm^{-2}	[88]
SWCNT	Covalent functionalization with 2-(2-thienyl)ethanol	5.00	Regioregular P3OT	N/A	N/A	Active layer	750.00	0.0095	NR	0.184	AM 1.5 G, 150 W	[118]
MWCNT	Oxidation (mix of H_2SO_4 and HNO_3)	1.00	P3HT	B	PCBM	Active layer	570.00	11.4700	61.300	4.100	AM 1.5 G, 95 mW cm^{-2}	[64]
MWCNT	Oxidation (mix of H_2SO_4 and HNO_3)	1.00	P3HT	N	PCBM	Active layer	550.00	10.4100	63.800	3.700	AM 1.5 G, 95 mW cm^{-2}	[64]
MWCNT	Oxidation (mix of H_2SO_4 and HNO_3)	1.00	P3HT	N/A	PCBM	Active layer	580.00	8.5200	65.300	3.200	AM 1.5 G, 95 mW cm^{-2}	[64]
MWCNT	Oxidation (mix of H_2SO_4 and HNO_3)	0.20	P3HT indene-C60 bisadduct	B and N	PCBM	Active layer	560.00	9.2900	57.500	3.000	AM 1.5 G, 95 mW cm^{-2}	[64]
MWCNT	Oxidation (mix of H_2SO_4 and HNO_3)	N/A	Poly(2-methoxy-5-(2′-ethylhexyloxy) 1-4-phenylenevinylene)	N	InP	Active layer	790.00	11.900	65.000	6.110	AM 1.5 G, 100 mW cm^{-2}	[58]
SWCNT	N/A	1:1	P3OT	N/A	N/A	Electron donor layer	400.00	0.0010	43.000	NR		[137]
SWCNT	Acid treatment, and then dispersed with SDS	1.00	P3HT	N/A	N/A	Active layer	750.00	0.5000	NR	NR	AM 1.5 G, 100 mW cm^{-2}	[138]
SWCNT	Oxidation (mix of H_2SO_4 and HNO_3)	N/A	P3HT	N/A	PCBM	Active layer	520.00	5.5300	0.490	1.800	80 mW cm^{-2}	[126]
SWCNT	Amidation with 2-aminothiophene	0.50	P3HT	N/A	PCBM	Photoactive layer	550.00	5.6000	0.580	1.780	AM 1.5 G, 100 mW cm^{-2}	[140]
MWCNT	Oxidation (mix of H_2SO_4 and HNO_3)	0.01	Regioregular P3HT	N/A	PCBM	Active layer	520.00	11.3300	54.620	3.470	AM 1.5 G, 100 mW cm^{-2}	[143]
SWCNT	Noncovalent functionalization with the polymer	N/A	Separate layer in the device	N/A	N/A	Donor layer	580.00	8.3600	69.350	3.360	AM 1.5 G	[147]
SWCNT	N/A	0.75	P3HT	N/A	N/A	Separate layer	509.63	8.2000	24.600	3.520	AM 1.5 G	[148]
SWCNT	N/A (nanotubes were semiconducting)	3.00	P3HT	N/A	N/A	Active layer	1040.00	1.9900	NR	0.720	AM 1.5 G	[149]
MWCNT	Oxidation (mix of H_2SO_4 and HNO_3)	0.04	Poly(3,4-ethylene dioxythiophene)	N/A	Polystyrene sulfonic acid	Active layer	560	9.0300	47.400	2.390	100 mW cm^{-2}, AM 1.5 G	[150]
DWCNT	37% HCl treatment	1.00	2,7-Bis-(3,3‴-didodecyl-[2,2′,5′,2″;5″,2‴] quaterthiophen-5-yl)-fluoren-9-one	N/A	PCBM	Active layer	530	2.3700	0.370	0.430	100 mW cm^{-2}	[151]

CNT, carbon nanotube; DWCNT, double-walled carbon nanotube; InP, Indium phosphate; MWCNT, multi-walled carbon nanotube; N/A, not applicable; P3HT, poly(3-hexylthiophene-1,3-diyl); P3OT, poly(3-octylthiophene); PCBM, (6,6)-phenyl-C_{61}-butyric-acid methyl ester; SWCNT, single-walled carbon nanotube.

is removed slowly from the solution and the liquid allowed to flow by gravity. A natural drying process follows, and the film coat on the substrate is formed.

3.2.5. Other printing techniques

Other techniques include gravure printing [132,133], flexographic printing [134], screen printing [135] and rotary screen printing [127]. They involve transferring the motif to a substrate by physical contact between the object carrying the motif and the substrate.

4. CASE STUDIES

There are several examples in the open literature where authors have investigated the use of CNTs in OSCs. Case studies where CNT/polymer composites have been used in the fabrication of OSCs are briefly highlighted, and some important developments in the field, based on SWCNTs, DWCNTs or MWCNTs as examples, are discussed in the subsequent section.

4.1. Single-walled carbon nanotubes

A composite consisting of a polycarbonate polymer and a 5 wt% loading of SWCNTs was found to increase the conductivity by four orders of magnitude compared with the pristine polymer [136]. SWCNTs combined with poly(2-methoxyl-5-(2-ethoxylhexyloxy)-1,4-phenylenevinylene) in the ratio 1:1 and with a V_{oc} of 0.4 V and J_{sc} of 1 μm A cm^{-1} achieved an FF of 43% [137]. A SWCNT composite with P3OT was synthesized to determine the effect of the SWCNT loading. A 15% loading was found to be the most favourable because the hole mobility increased 500 times compared with pristine P3OT [138]. Acid-functionalized SWCNTs were found to enhance the conjugation length of P3HT, thereby improving the absorption capacity. A device fabricated from these materials had a photoconversion of ~1.8% [126]. SWCNTs when combined with P3HT-*b*-PS formed a device with increased photoresponse. This could be attributed to enhanced exciton dissociation and charge carrier separation [139]. Acid-treated SWCNTs covalently combined with aminothiophene through amide bonds to form a SWCNT–CONHTh composite showing an efficiency of 1.78%, while the pristine SWCNTs had an efficiency of 1.48% and thiophene without SWCNT had an efficiency of 1% [140]. Integration of SWCNTs by simple and direct thermocompression in a polyethylene polymer formed a composite with good optical transparency and conductivity [141]. When SWCNTs formed a composite with P3HT, charge carriers were found to be long-lived in the polymer matrix owing to the improved interfacial electron transfer [142].

4.2. Double-walled carbon nanotubes

Double-walled CNT/P3OT composite conductivities were compared with CNT loadings between 1% and 20% to determine the suitability of the composite as a photoactive material. The conductivity increased with CNT loading, and 20% was reported to have the highest conductivity of 1.52×10^{-3} S cm^{-1}. The high conductivity of the composite makes it suitable for use as a photoactive layer in a PV cell [121]. Inclusion of DWCNTs in the active layer consisting of P3HT/C-60 increased the performance of the cell owing to increased charge transport and reduced recombination [59].

4.3. Multi-walled carbon nanotubes

A composite of MWCNTs and doped polyaniline (PANI) in its emeraldine salt was synthesized by *in situ* polymerization. The conductivity increased by 50–70% compared with pristine PANI. The increase was attributed to the presence of carboxylic acid groups on the walls of the MWCNTs, which improved dispersion [143]. To determine the best MWCNT loading in the polymer matrix for efficient conductivity, a composite of PANI and MWCNTs was synthesized by oxidative *in situ* polymerization. A 2 wt% loading of acid-functionalized MWCNTs gave the highest conductivity [144]. Polymer composites of poly(3,4-dihexyloxythiophene) and poly(3,4-dimethyloxythiophene-co-3,4-dihexyloxythiophene) with MWCNTs, conjugated by low energy band gap, were synthesized. A high conductivity of 16 S cm^{-1} was attained at 30% loading [38]. Sulfonated PANI forms a water-soluble and conducting composite with MWCNTs that was surface functionalized with phenylamine groups by *in situ* polymerization. The conductivity increased by two orders of magnitude compared with that of pristine MWCNTs [145]. A composite of pristine MWCNTs and poly[(2-methoxy-5-(2′-etheylhexyloxy)-1,4-phenylene] was formed by solution mixing [146]. Photoluminescence quenching and increased absorbance were some of the attributes of the composite formed. The electrical conductivity threshold of this composite was noted at 0.5% MWCNT loading; however, higher loading than this formed a dense network of nanotubes that acted as a nanomeric heat sink. Additional examples are given in Table II.

5. CONCLUSION

From the discussion, CNT/polymer composites have been shown to possess improved mechanical, conduction and electrical properties than the original polymer from which they were made. CNTs have also been found to enhance OSC efficiency owing to the improved dissociation of excitons and electron transfer to the electrodes. However, these efficiencies are still very low when compared with SSCs, and more research is required to improve on the same. The research should focus more on the synthesis of copolymers, whose absorption will cover a wider range of the solar spectrum and with improved environmental stability, which is another challenge in OSCs. Further research is also required on the synthesis of CNTs, especially SWCNTs, to ensure metallic conductors and semiconductors are synthesized as different products. When the

Int. J. Energy Res. 2014; **38**:1635–1653 © 2014 John Wiley & Sons, Ltd.
DOI: 10.1002/er

product is a mixture of metallic conductors and semiconductors, postsynthesis separation is difficult. In addition, when a mixture of the two is used to form a composite for OSCs, the metallic type is reported to short circuit, thereby lowering efficiency. Easier and more efficient methods of synthesizing DWCNTs also need to be explored. Doped CNTs in polymer composites could be better conductors than pristine CNTs when used in OSCs and, thus, should be intensively investigated as currently data on these are limited.

ACKNOWLEDGEMENTS

The authors thank the University of KwaZulu-Natal (UKZN), the National Research Foundation and the India, Brazil and South Africa energy project for financial assistance. G. Keru thanks the UKZN College of Agriculture, Engineering and Science for the award of a postgraduate bursary. We are grateful to Prof B. S. Martincigh for her critical comments and also for proofreading the manuscript.

REFERENCES

1. Pegels A. Renewable energy in South Africa: potentials, barriers and options for support. *Energy Policy* 2010; **38**:4945–4954.
2. Spolding-Fecher R, Winker H, Mwakasonda S. Energy and the world summit on sustainable development. What next? *Energy Policy* 2005; **33**:99–112.
3. Miah D, Ahmed R, Beleal MU. Biomass fuel use by the rural households in Chittagong region, Bangladesh. *Biomass and Bioenergy* 2003; **24**:277–283.
4. Posten C, Schaub G. Microalgae and terrestrial biomass as source for fuels. A process view. *Journal of Biotechnology* 2009; **142**:64–69.
5. Haehnlein S, Bayer P, Blum P. International legal status of the use of shallow geothermal energy. *Renewable and Sustainable Energy Reviews* 2010; **14**:2611–2625.
6. Lund JW, Freeston DH, Boyd TL. Direct utilization of geothermal energy 2010 worldwide review. *Geothermics* 2011; **40**:159–180.
7. Solangi KH, Islam MR, Saidur R, Rahim NA, Fayaz H. A review on global solar energy policy. *Renewable and Sustainable Energy Reviews* 2011; **15**:2149–2163.
8. Sesto E, Casale C. Exploitation of wind as an energy source to meet the world's electricity demand. *Journal of Wind Engineering and Industrial Aerodynamics* 1998; **74–76**:375–387.
9. Bhutto AW, Bazmi AA, Zahedi G. Greener energy: issues and challenges for Pakistan wind power prospective. *Renewable and Sustainable Energy Reviews* 2013; **20**:519–538.
10. Yüksel I. Hydropower for sustainable water and energy development. *Renewable and Sustainable Energy Reviews* 2010; **14**:462–469.
11. Gokcol C, Dursun B, Alboyaci B, Sunan E. Importance of biomass energy as alternative to other sources in Turkey. *Energy Policy* 2009; **37**:424–431.
12. Farhat AAM, Ugursal VI. Greenhouse gas emission intensity factors for marginal electricity generation in Canada. *International Journal of Energy Research* 2010; **34**:1309–1327.
13. Asim N, Kamaruzzaman S, Shideh A, Kasra S, Alghoul MA, Saadatian O, Zaidi SA. Review on the role of materials science in solar cells. *Renewable and Sustainable Energy Reviews* 2012; **16**:5834–5847.
14. Davidson O. Energising Africa. *Science in Africa*, 2009. Available from: http://www.scienceinafrica.com [30 March 2013]
15. Lewis NS, Nocera DG. Powering the planet: chemical challenges in solar energy utilization. *Proceedings of the National Academy of Sciences* 2006; **103**:15729–15735.
16. Wang C, Abdul-Rahman H, Rao SP. A new design of luminescent solar concentrator and its trial run. *International Journal of Energy Research* 2010; **34**:1372–1385.
17. Huang X, Han S, Huang W, Liu X. Enhancing solar cell efficiency the search for luminescent materials as spectral converters. *Chemical Society Reviews* 2013; **42**:173–201.
18. Zhang X, Wang X, Xiao H, Yang C, Ran J, Wang C, Hou Q, Li J. Simulation of $In_{0.65}Ga_{0.35}N$ single-junction solar cell. *Journal of Physics D: Applied Physics* 2007; **40**:7335–7338.
19. Matin MA, Mannir-Aliyu M, Quadery AH, Amin N. Prospects of novel front and back contacts for high efficiency cadmium telluride thin film solar cells from numerical analysis. *Solar Energy Materials and Solar Cells* 2010; **94**:1496–1500.
20. Choi SJ, Yu GJ, Kang GH, Lee JC, Kim D, Song H-E. The electrical properties and hydrogen passivation effect in mono crystalline silicon solar cell with various pre-deposition times in doping process. *Renewable Energy* 2013; **54**:96–100.
21. Kwon TY, Yang DH, Ju MK, Jung WW, Kim SY, Lee YW, Gong DY, Yi J. Screen printed phosphorus diffusion for low-cost and simplified industrial monocrystalline silicon solar cells. *Solar Energy Materials and Solar Cells* 2011; **95**:14–17.
22. Yahia IS, Yakuphanoglu F, Azim OA. Unusual photocapacitance properties of a mono-crystalline silicon solar cell for optoelectronic applications. *Solar Energy Materials and Solar Cells* 2011; **95**:2598–2605.

23. Yang B, Lee M. Fabrication of honeycomb texture on poly-Si by laser interference and chemical etching. *Applied Surface Science* 2013; **284**:565–568.
24. Xue C, Rao J, Varlamov S. A novel silicon nanostructure with effective light trapping for polycrystalline silicon thin film solar cells by means of metal-assisted wet chemical etching. *Physica Status Solidi (A) Applications and Materials Science* 2013; **210**:2588–2591. doi:10.1002/pssa.201330204.
25. Misra S, Yu L, Foldyna M, Roca i Cabarrocas P. High efficiency and stable hydrogenated amorphous silicon radial junction solar cells built on VLS-grown silicon nanowires. *Solar Energy Materials and Solar Cells* 2013; **118**:90–95.
26. Jovanov V, Xu X, Shrestha S, Schulte M, Hüpkes J, Zeman M, Knipp D. Influence of interface morphologies on amorphous silicon thin film solar cells prepared on randomly textured substrates. *Solar Energy Materials and Solar Cells* 2013; **112**:182–189.
27. Adomaitis RA, Schwarm A. Systems and control challenges in photovoltaic manufacturing processes: a modeling strategy for passivation and antireflection films. *Computers & Chemical Engineering* 2013; **51**:65–76.
28. Braga AFB, Moreira SP, Zampieri PR, Bacchin JMG, Mei PR. New processes for the production of solar-grade polycrystalline silicon: a review. *Solar Energy Materials and Solar Cells* 2008; **92**:418–424.
29. Pizzini S. Towards solar grade silicon: challenges and benefits for low cost photovoltaics. *Solar Energy Materials and Solar Cells* 2010; **94**:1528–1533.
30. Abdulrazzaq OA, Saini V, Bourdo S, Dervishi E, Biris AS. Organic solar cells: a review of materials, limitations, and possibilities for improvement. *Particulate Science and Technology* 2013; **31**:427–442.
31. Jeon SO, Lee JY. Improved lifetime in organic solar cells using a bilayer cathode of organic interlayer/Al. *Solar Energy Materials and Solar Cells* 2012; **101**:160–165.
32. Deibel C, Strobel T, Dyakonov V. Role of the charge transfer state in organic donor–acceptor solar cells. *Advanced Materials* 2010; **22**:4097–4111.
33. Janssen RAJ, Nelson J. Factors limiting device efficiency in organic photovoltaics. *Advanced Materials* 2012; **25**(13):1847–1858.
34. Jørgensen M, Norrman K, Gevorgyan SA, Tromholt T, Andreasen B, Krebs FC. Stability of polymer solar cells. *Advanced Materials* 2012; **24**:580–612.
35. Scharber MC, Mühlbacher D, Koppe M, Denk P, Waldauf C, Heeger AJ, Brabec CJ. Design rules for donors in bulk-heterojunction solar cells towards 10% energy conversion efficiency. *Advanced Materials* 2006; **18**:789–794.
36. Weickert J, Dunbar RB, Hesse HC, Wiedemann W, Schmidt-Mende L. Nanostructured organic and hybrid solar cells. *Advanced Materials* 2011; **23**:1810–1828.
37. Kim TH, Yang SJ, Park CY. Carbon nanomaterials in organic photovoltaic cells. *Carbon Letters* 2011; **12**:194–206.
38. Liu Z, He D, Wang Y, Wu H, Wang J, Wang H. Improving photovoltaic properties by incorporating both SPFGraphene and functionalized multi-walled carbon nanotubes. *Solar Energy Materials and Solar Cells* 2010; **94**:2148–2153.
39. Skompska M. Hybrid conjugated polymer/semiconductor photovoltaic cells. *Synthetic Metals* 2010; **160**:1–15.
40. Jørgensen M, Norrman K, Krebs FC. Stability/degradation of polymer solar cells. *Solar Energy Materials and Solar Cells* 2008; **92**:686–714.
41. Peters CH, Sachs-Quintana IT, Mateker WR, Heumueller T, Rivnay J, Noriega R, Beiley ZM, Hoke ET, Salleo A, McGehee MD. The mechanism of burn-in loss in a high efficiency polymer solar cell. *Advanced Materials* 2012; **24**:663–668.
42. Williams G, Wang Q, Aziz H. The photo-stability of polymer solar cells: contact photo-degradation and the benefits of interfacial layers. *Advanced Functional Materials* 2013; **23**:2239–2247.
43. Wang DH, Moon JS, Seifter J, Jo J, Park JH, Park OO, Heeger AJ. Sequential processing: control of nanomorphology in bulk heterojunction solar cells. *Nano Letters* 2011; **11**:3163–3168.
44. Price SC, Stuart AC, Yang L, Zhou H, You W. Fluorine substituted conjugated polymer of medium band gap yields 7% efficiency in polymer-fullerene solar cells. *Journal of the American Chemical Society* 2011; **133**:4625–4631.
45. Cox M, Gorodetsky A, Kim B, Kim KS, Jia Z, Kim P, Nuckolls C, Kymissis I. Single-layer graphene cathodes for organic photovoltaics. *Applied Physics Letters* 2011; **98**:123303.
46. Park SH, Roy A, Beaupre S, Cho S, Coates N, Moon JS, Moses D, Leclerc M, Lee K, Heeger AJ. Bulk heterojunction solar cells with internal quantum efficiency approaching 100%. *Nature Photonics* 2009; **3**:297–302.
47. Zhang Y, Basel TP, Gautam BR, Yang X, Mascaro DJ, Liu F, Vardeny ZV. Spin-enhanced organic bulk heterojunction photovoltaic solar cells. *Nature Communications* 2012; **3**:1043.
48. Ye Q, Chi C. Conjugated polymers for organic solar cells. In *Solar Cells—New Aspects and Solutions*, Kosyachenko LA (ed.). InTech: Rijeka, 2011; 453–476. ISBN: 978-953-307-761-1, DOI: 10.5772/23275. Available from: http://www.intechopen.com/books/solar-cells-new-aspects-and-solutions/conjugated-polymers-for-organic-solar-cells

49. Somani SP, Somani PR, Umeno M, Flahaut E. Improving photovoltaic response of poly(3-hexylthiophene)/*n*-Si heterojunction by incorporating double-walled carbon nanotubes. *Applied Physics Letters* 2006; **89**:223505,1-2.
50. Ferguson AJ, Blackburn JL, Kopidakis N. Fullerenes and carbon nanotubes as acceptor materials in organic photovoltaics. *Materials Letters* 2013; **90**:115–125.
51. Kim YH, Müller-Meskamp L, Zakhidov AA, Sachse C, Meiss J, Bikova J, Cook A, Zakhidov AA, Leo K. Semi-transparent small molecule organic solar cells with laminated free-standing carbon nanotube top electrodes. *Solar Energy Materials and Solar Cells* 2012; **96**:244–250.
52. Tune DD, Flavel BS, Quinton JS, Ellis AV, Shapter JG. Single-walled carbon nanotube network electrodes for dye solar cells. *Solar Energy Materials and Solar Cells* 2010; **94**:1665–1672.
53. Xu F, Zhu WQ, Yan L, Xu H, Xiong LH, Li JH. Single-walled carbon nanotube anodes based high performance organic light-emitting diodes with enhanced contrast ratio. *Organic Electronics* 2012; **13**:302–308.
54. Aitola K, Borghei M, Kaskela A, Kemppainen E, Nasibulin AG, Kauppinen EI, Lund PD, Ruiz V, Halme J. Flexible metal-free counter electrode for dye solar cells based on conductive polymer and carbon nanotubes. *Journal of Electroanalytical Chemistry* 2012; **683**:70–74.
55. Aitola K, Halme J, Feldt S, Lohse P, Borghei M, Kaskela A, Nasibulin AG, Kauppinen EF, Lund PD, Bachloo G, Hagfedt A. Highly catalytic carbon nanotube counter electrode on plastic for dye solar cells utilizing cobalt-based redox mediator. *Electrochimica Acta* 2013; **111**:206–209.
56. Arena A, Daonato N, Saitta G. Photovoltaic properties of multi-walled carbon nanotubes. *Microelectronic Journal* 2008; **39**:1659–1662.
57. Keru G, Ndungu PG, Nyamori VO. Nitrogen-doped carbon nanotubes synthesised by pyrolysis of (4-{[(pyridine-4-yl)methylidene]amino}phenyl)ferrocene. *Journal of Nanomaterials* 2013; **2013**:1–7.
58. Lee JM, Kwon BH, Park HI, Kim H, Kim MG, Park JS, Yoo S, Jeon DY, Kim SO. Exciton dissociation and charge-transport enhancement in organic solar cells with quantum-dot/N-doped CNT hybrid nanomaterials. *Advanced Materials* 2013; **25**:2011–2017.
59. Somani SP, Somani PR, Umeno M. Carbon nanotube incorporation: a new route to improve the performance of organic-inorganic heterojunction solar cells. *Diamond and Related Materials* 2008; **17**:585–588.
60. Cataldo S, Salice P, Menna E, Pignataro B. Carbon nanotubes and organic solar cells. *Energy & Environmental Science* 2012; **5**:5919–5940.
61. Guenes S, Neugebauer H, Sariciftci NS. Conjugated polymer-based organic solar cells. *Chemical Reviews* 2007; **107**:1324–1338.
62. Bhattacharyya S, Kymakis E, Amaratunga GAJ. Photovoltaic properties of dye functionalized single-wall carbon nanotube/conjugated polymer devices. *Chemistry of Materials* 2004; **16**:4819–4823.
63. Hwang SK, Lee JM, Kim S, Park JS, Park HI, Ahn CW, Lee KJ, Lee T, Kim SO. Flexible multilevel resistive memory with controlled charge trap band N-doped carbon nanotubes. *Nano Letters* 2012; **12**:2217–2221.
64. Lee JM, Park JS, Lee SH, Kim H, Yoo S, Kim SO. Selective electron- or hole-transport enhancement in bulk heterojunction organic solar cells with N- or B-doped carbon nanotubes. *Advanced Materials* 2011; **23**:629–633.
65. Jana D, Sun C-L, Chen L-C, Chen K-H. Effect of chemical doping of boron and nitrogen on the electronic, optical, and electrochemical properties of carbon nanotubes. *Progress in Materials Science* 2013; **58**:565–635.
66. Iijima S, Ichihashi T. Single-shell carbon nanotubes of 1-nm diameter. *Nature* 1993; **363**:603–605.
67. Guo T, Nikolaev P, Thess A, Colbert DT, Smalley RE. Catalytic growth of single-walled nanotubes by laser vaporization. *Chemical Physics Letters* 1995; **243**:49–54.
68. Allouche H, Monthioux M, Jacobsen RL. Chemical vapor deposition of pyrolytic carbon on carbon nanotubes: part 1. Synthesis and morphology. *Carbon* 2003; **41**:2897–2912.
69. Danafar F, Fakhru'l-Razi A, Mohd-Salleh MA, Awang-Biak DR. Influence of catalytic particle size on the performance of fluidized-bed chemical vapor deposition synthesis of carbon nanotubes. *Chemical Engineering Research and Design* 2011; **89**:214–223.
70. Kumar M. Carbon nanotube synthesis and growth mechanism. In *Carbon Nanotubes—Synthesis, Characterization, Applications*, Yellampalli S (ed.). In Tech: Rijeka, 2011. ISBN: 978-953-307-497-9, DOI: 10.5772/19331
71. Bondi SN, Lackey WJ, Johnson RW, Wang X, Wang ZL. Laser assisted chemical vapor deposition synthesis of carbon nanotubes and their characterization. *Carbon* 2006; **44**:1393–1403.
72. Kymakis E, Amaratunga GAJ. Single-wall carbon nanotube conjugated polymer photovoltaic devices. *Applied Physics Letters* 2002; **80**:112–114.
73. Endo M, Strano MS, Ajayan PM. Carbon nanotubes. In *Topics in Applied Physics*, Jorio A, Dresselhaus MS (eds). Springer: Berlin, 2008; 13–62.

74. Coleman JN, Khan U, Blau WJ, Gun'ko YK. Small but strong: a review of the mechanical properties of carbon nanotube/polymer composites. *Carbon* 2006; **44**:1624–1652.
75. Kim D-Y, Yun YS, Bak H, Cho SY, Jin H-J. Aspect ratio control of acid modified multi-walled carbon nanotubes. *Current Applied Physics* 2010; **10**:1046–1052.
76. Endo M, Haruyashi T, Kim YA, Terrones M, Dresselhaus MS. Applications of carbon nanotubes. *Philosophical Transactions Royal Society London A* 2004; **362**:2223–2238.
77. Oosthuzen RS, Nyamori VO. Carbon nanotubes as support for palladium and bimetallic catalyst for use in hydrogenation reactions. *Platinum Metals Review* 2011; **55**:154–169.
78. Harris PJF. Carbon nanotube composites. *International Materials Reviews* 2004; **49**:31–43.
79. Jones WE Jr, Chiguma J, Johnson E, Pachamuthu A, Santos D. Electrically and thermally conducting nanocomposites for electronic applications. *Materials* 2010; **3**:1478–1496.
80. Mohlala MS, Liu X-Y, Coville NJ. Synthesis of multi-walled carbon nanotubes catalyzed by substituted ferrocenes. *Journal of Organometallic Chemistry* 2006; **691**:4768–4772.
81. Dubacheva GV, Liang C-K, Bassani DM. Functional monolayers from carbon nanostructures (fullerenes, carbon nanotubes, and graphene) as novel materials for solar energy conversion. *Coordination Chemistry Reviews* 2012; **256**:2628–2639.
82. Guldi DM, Costa RD. Nanocarbon hybrids: the paradigm of nanoscale self-ordering/self-assembling by means of charge transfer/doping interactions. *The Journal of Physical Chemistry Letters* 2013; **4**:1489–1501.
83. Kanemitsu Y. Multiple exciton generation and recombination in carbon nanotubes and nanocrystals. *Accounts of Chemical Research* 2013; **46**(6):1358–1366.
84. Sliaužys G, Arlauskas K, Gulbinas V. Photogeneration and recombination of charge carrier pairs and free charge carriers in polymer/fullerene bulk heterojunction films. *Physica Status Solidi A* 2012; **209**:1302–1306.
85. Bauhofer W, Kovacs JZ. A review and analysis of electrical percolation in carbon nanotube polymer composites. *Composites Science and Technology* 2009; **69**:1486–1498.
86. Yang MJ, Koutsos V, Zaiser M. Interactions between polymers and carbon nanotubes: a molecular dynamics study. *Journal of Physical Chemistry B* 2005; **109**:10009–10014.
87. Jun GH, Jin SH, Park SH, Jeon S, Hong SH. Highly dispersed carbon nanotubes in organic media for polymer : fullerene photovoltaic devices. *Carbon* 2012; **50**:40–46.
88. Li C, Chen Y, Wang Y, Iqbal Z, Chhowalla M, Mitra S. A fullerene-single-wall carbon nanotube complex for polymer bulk heterojunction photovoltaic cells. *Journal of Materials Chemistry* 2007; **17**:2406–2411.
89. Laird ED, Li CY. Structure and morphology control in crystalline colymer carbon nanotube nanocomposites. *Macromolecules* 2013; **46**:2877–2891.
90. Ruoff RS, Qian D, Liu WK. Mechanical properties of carbon nanotubes theoretical predictions. *Comptes Rendus Physique* 2003; **4**:993–1008.
91. Shokrieh MM, Rafiee R. A review of the mechanical properties of isolated carbon nanotubes and carbon nanotube composites. *Mechanics Composite Materials* 2010; **46**:155–172.
92. Iijima S, Brabec C, Maiti A, Bernholc J. Structural flexibility of carbon nanotubes. *Journal of Chemistry and Physics* 1996; **104**:2089–2092.
93. Lin Y, Zhou B, Fernando KAS, Liu P, Allard LF, Sun YP. Polymeric carbon nanocomposites from carbon nanotubes functionalized with matrix polymer. *Macromolecules* 2003; **36**:7199–7204.
94. Sakellariou G, Priftis D, Baskaran D. Surface-initiated polymerization from carbon nanotubes: strategies and perspectives. *Chemical Society Reviews* 2013; **42**:677–704.
95. Padgett CW, Brenner DW. Influence of chemisorption on the thermal conductivity of single-wall carbon nanotube. *Nano Letters* 2004; **4**:1051–1053.
96. Han Z, Fina A. Thermal conductivity of carbon nanotubes and their polymer nanocomposites: a review. *Progress in Polymer Science* 2011; **36**:914–944.
97. Lin T, Bajpai V, Ji T, Dai LM. Chemistry of carbon nanotubes. *Australian Journal of Chemistry* 2003; **56**:635–651.
98. Ozin GA, Arsenault AC. Nanochemistry: a chemical approach to nanomaterials. *Materials Today* 2009; **12**:46.
99. Aqel A, El-Nour KMMA, Ammar RAA, Al-Warthan A. Carbon nanotubes, science and technology part (I) structure, synthesis and characterisation. *Arabian Journal of Chemistry* 2012; **5**:1–23.
100. Rong H, Liu Z, Wu Q, Lee Y-H. A facile and efficient gas phase process for purifying single-walled carbon nanotubes. *Current Applied Physics* 2010; **10**:1231–1235.
101. Edwards ER, Antunes EF, Botelho EC, Baldan MR, Corat EJ. Evaluation of residual iron in carbon nanotubes purified by acid treatments. *Applied Surface Science* 2011; **258**:641–648.
102. Hou P-X, Liu C, Cheng H-M. Purification of carbon nanotubes. *Carbon* 2008; **46**:2003–2025.
103. Andrews R, Jacques D, Qian D, Dickey EC. Purification and structural annealing of multi-walled carbon

nanotubes at graphitization temperatures. *Carbon* 2001; **39**:1681–1687.
104. Serp P, Corrias M, Kalck P. Carbon nanotubes and nanofibers in catalysis. *Applied Catalysis A: General* 2003; **253**:337–358.
105. Ma PC, Siddiqui NA, Marom G, Kim JK. Dispersion and functionalization of carbon nanotubes for polymer-based nanocomposites: a review. *Composites Part A: Applied Science and Manufacturing* 2010; **41**:1345–1367.
106. Park C, Ounaies Z, Watson KA, Crooks RE, Smith J Jr, Lowther SE, Connell JW, Siochi JE, Harrison JS, St Clair TL. Dispersion of single-wall carbon nanotubes by *in situ* polymerization under sonication. *Chemical Physics Letters* 2002; **364**:303–308.
107. Zhang M, Su L, Mao L. Surfactant functionalization of carbon nanotubes (CNTs) for layer-by-layer assembling of CNT multi-layer films and fabrication of gold nanoparticle/CNT nanohybrid. *Carbon* 2006; **44**:276–283.
108. Alpatova AL, Shan W, Babica P, Upham BL, Rogensues AR, Masten SJ, Drown E, Mohanty AK, Alocilja EC, Tarabara VV. Single-walled carbon nanotubes dispersed in aqueous media via non-covalent functionalization: effect of dispersant on the stability, cytotoxicity, and epigenetic toxicity of nanotube suspensions. *Water Research* 2010; **44**:505–520.
109. Liu P. Modifications of carbon nanotubes with polymers. *European Polymer Journal* 2005; **41**:2693–2703.
110. Yang ZL, Pu HT, Yin YL. Covalent functionalization of multi-walled carbon nanotubes by polyvinylimidazole. *Materials Letters* 2005; **59**:2838–2841.
111. Jin F-L, Yop-Rhee K, Park S-J. Functionalization of multi-walled carbon nanotubes by epoxide ring-opening polymerization. *Journal of Solid State Chemistry* 2011; **184**:3253–3256.
112. Kónya Z, Vesselenyi I, Niesz K, Kukovecz A, Demortier A, Fonseca A, Dehelle J, Mekhalif Z, B-Naggy J, Ko s AA, Osvàth Z, Kocsonya A, Bir LP, Kiricsi I. Large scale production of short functionalized carbon nanotubes. *Chemical Physics Letters* 2002; **360**:429–435.
113. Chen L, Pang X-J, Zhang Q-T, Yu Z-l. Cutting of carbon nanotubes by a two-roller mill. *Materials Letters* 2006; **60**:241–244.
114. Kalita G, Adhikari S, Aryal HR, Afre R, Soga T, Sharon M, Umeno M. Functionalization of multi-walled carbon nanotubes with nitrogen plasma for photovoltaic device application. *Current Applied Physics* 2009; **9**:346–351.
115. Spitalsky Z, Tasis D, Papagelis K, Galiotis C. Carbon nanotube/polymer composites: chemistry, processing, mechanical and electrical properties. *Progress in Polymer Science* 2010; **35**:357–401.
116. Rahmat M, Hubert P. Carbon nanotube–polymer interactions in nanocomposites: a review. *Composites Science and Technology* 2011; **72**:72–84.
117. Geng J, Zeng T. Influence of single-walled carbon nanotubes induced crystallinity enhancement and morphology change on polymer photovoltaic devices. *Journal of the American Chemical Society* 2006; **128**:16827–16833.
118. Nogueira AF, Lomba BS, Soto-Oviedo MA, Correia CRD, Corio P, Furtado CA, Hummelgen IA. Polymer solar cells using single-wall carbon nanotubes modified with thiophene pedant groups. *Journal of Physical Chemistry C* 2007; **111**:18431–18438.
119. Al-Saleh MH, Sundararaj U. Morphological, electrical and electromagnetic interference shielding characterization of vapour grown carbon nanofiber/polystyrene nanocomposites. *Polymer International* 2013; **62**:601–607.
120. Socher R, Krause B, Hermasch S, Wursche R, Pötschke P. Electrical and thermal properties of polyamide 12 composites with hybrid fillers systems of multi-walled carbon nanotubes and carbon black. *Composites Science and Technology* 2011; **71**:1053–1059.
121. Koizhaiganova R, Kim HJ, Vasudevan T, Kudaibergenov S, Lee MS. *In situ* polymerization of 3-hexylthiophene with double-walled carbon nanotubes: studies on the conductive nanocomposite. *Journal of Applied Polymer Science* 2010; **115**:2448–2454.
122. Kim HJ, Koizhaiganova R, Vasudevan T, Sanjeeviraja C, Lee MS. Single step synthesis of poly(3-oc tylthiophene)/multi-walled carbon nanotube composites and their characterizations. *Polymers for Advanced Technologies* 2009; **20**:736–741.
123. Wengeler L, Schmidt-Hansberg B, Peters K, Scharfer P, Schabel W. Investigations on knife and slot die coating and processing of polymer nanoparticle films for hybrid polymer solar cells. *Chemical Engineering and Processing Process Intensification* 2011; **50**:478–482.
124. Nagata S, Atkinson GM, Pestov D, Tepper GC, McLeskey JT Jr. Co-planar bi-metallic interdigitated electrode substrate for spin-coated organic solar cells. *Solar Energy Materials and Solar Cells* 2011; **95**:1594–1597.
125. Vairavan R, Mohamad Shahimin M, Juhari N. Fabrication and characterisation of MEH-PPV/CdTe/CdS. *Solar Cell* 2011; 454–458. DOI: 10.1109/CHUSER.2011.6163772 [15 February 2013].
126. Singh RK, Kumar J, Kumar A, Kumar V, Kant R, Singh R. Poly(3-hexylthiophene): functionalized single-walled carbon nanotubes: (6,6)-phenyl-C-$_{61}$-

butyric acid methyl ester composites for photovoltaic cell at ambient condition. *Solar Energy Materials and Solar Cells* 2010; **94**:2386–2394.
127. Sondergaard R, Hosel M, Angmo D, Larsen-olsen TT, Krebs FC. Roll-to-roll fabrication of thin film. *Materials Today* 2012; **15**:37–49.
128. Girotto C, Rand BP, Genoe J, Heremans P. Exploring spray coating as a deposition technique for the fabrication of solution-processed solar cells. *Solar Energy Materials and Solar Cells* 2009; **93**:454–458.
129. Peh RJ, Lu Y, Zhao F, Lee C-LK, Kwan WL. Vacuum-free processed transparent inverted organic solar cells with spray-coated PEDOT:PSS anode. *Solar Energy Materials and Solar Cells* 2011; **95**:3579–3584.
130. Kang J-W, Kang Y-J, Jung S, Song M, Kim D-G, Su Kim C, Su Kim C, Chang SK, Kim SH. Fully spray-coated inverted organic solar cells. *Solar Energy Materials and Solar Cells* 2012; **103**:76–79.
131. Hu Z, Zhang J, Xiong S, Zhao Y. Performance of polymer solar cells fabricated by dip coating process. *Solar Energy Materials and Solar Cells* 2012; **99**:221–225.
132. Kopola P, Aernouts T, Guillerez S, Jin H, Tuomikoski M, Maaninen A, Hast J. High efficient plastic solar cells fabricated with a high-throughput gravure printing method. *Solar Energy Materials and Solar Cells* 2010; **94**:1673–1680.
133. Kopola P, Aernouts T, Sliz R, Guillerez S, Ylikunnari M, Cheyns D, Valimaki M, Tuomikoski M, Hast J, Jabbour G, Myllya R, Maaninen A. Gravure printed flexible organic photovoltaic modules. *Solar Energy Materials and Solar Cells* 2011; **95**:1344–1347.
134. Krebs FC, Fyenbo J, Jorgensen M. Product integration of compact roll-to-roll processed polymer solar cell modules: methods and manufacture using flexographic printing, slot die coating and rotary screen printing. *Journal of Materials Chemistry* 2010; **20**:8994–9001.
135. Krebs FC, Jørgensen M, Norrman K, Hagemann O, Alstrup J, Nielsen TD, Fyenbo J, Larsen K, Kristensen J. A complete process for production of flexible large area polymer solar cells entirely using screen printing—first public demonstration. *Solar Energy Materials and Solar Cells* 2009; **93**:422–441.
136. Pradhan B, Kohlmeyer RR, Chen J. Fabrication of in-plane aligned carbon nanotube–polymer composite thin films. *Carbon* 2010; **48**:217–222.
137. Ltaief A, Bouazizi A, Davenas J. Charge transport in carbon nanotubes–polymer composite photovoltaic cells. *Materials* 2009; **2**:710–718.
138. Kymakis E, Servati P, Tzanetakis P, Koudoumas E, Kornilios N, Rompogiannakis I, Franghiadakis Y, Amaratunga GAJ. Effective mobility and photocurrent in carbon nanotube–polymer composite photovoltaic cells. *Nanotechnology* 2007; **18**:435702.
139. Sarker BK, Arif M, Khondaker SI. Near-infrared photoresponse in single-walled carbon nanotube/polymer composite films. *Carbon* 2010; **48**:1539–1544.
140. Stylianakis MM, Mikroyannidis JA, Kymakis E. A facile, covalent modification of single-wall carbon nanotubes by thiophene for use in organic photovoltaic cells. *Solar Energy Materials and Solar Cells* 2010; **94**:267–274.
141. Nasibulin AG, Ollikainen A, Anisimov AS, Brown DP, Pikhitsa PV, Holopainen S, Penttila JS, Helisto P, Ruokohainen J, Choi M, Kauppinen EI. Integration of single-walled carbon nanotubes into polymer films by thermo-compression. *Chemical Engineering Journal* 2008; **136**:409–413.
142. Ferguson AJ, Blackburn JL, Holt JM, Kopidakis N, Tenent RC, Barnes TM, Heben JM, Rumble G. Photoinduced energy and charge transfer in P3HT : SWNT composites. *Journal of Physical Chemistry Letters* 2010; **1**:2406–2411.
143. Wu M-C, Lin Y-Y, Chen S, Liao H-C, Wu Y-J, Chen C-W, Chen Y-F, Su W-F. Enhancing light absorption and carrier transport of P3HT by doping multi-wall carbon nanotubes. *Chemical Physics Letters* 2009; **468**:64–68.
144. Choudhury A, Kar P. Doping effect of carboxylic acid group functionalized multi-walled carbon nanotube on polyaniline. *Composites Part B: Engineering* 2011; **42**:1641–1647.
145. Xu J, Yao P, Li X, He F. Synthesis and characterization of water-soluble and conducting sulfonated polyaniline/para-phenylenediamine-functionalized multi-walled carbon nanotubes nano-composite. *Materials Science and Engineering B* 2008; **151**:210–219.
146. Bansal M, Srivastava R, Lal C, Kamalasanan MN, Tanwar LS. Low electrical percolation threshold and PL quenching in solution-blended MWNT-MEH PPV nanocomposites. *Journal of Experimental Nanoscience* 2010; **5**:412–426.
147. Dabera GDMR, Jayawardena KDGI, Prabhath MRR, Yahya I, Tan YY, Nismy NA, Shiozawa H, Sauer M, Ruiz-Soria G, Ayala P, Stojan V, Domitha AA, Jorowski PO, Pichler PD, Silva SRP. Hybrid carbon nanotube networks as efficient hole extraction layers for organic photovoltaics. *American Chemical Society Nano* 2013; **7**:556–565.
148. Mallajosyula AT, Kumar S, Iyer S, Mazhari B. Increasing the efficiency of charge extraction limited poly-(3-hexylthiophene):[6,6] phenyl C61 butyric acid methyl ester solar cells using single-walled

carbon nanotubes with metallic characteristics. *Journal of Applied Physics* 2011; **109**:124908–124910.

149. Ren S, Bernardi M, Lunt RR, Bulovic V, Grossman JC, Gradečak S. Toward efficient carbon nanotube/P3HT solar cells: active layer morphology, electrical, and optical properties. *Nano Letters* 2011; **11**:5316–5321.
150. Li J, Liu J, Gao C, Chen G. Nanocomposite hole-extraction layers for organic solar cells. *International Journal of Photoenergy* 2011; **2011**:Article ID 392832;1–5.
151. Picard L, Lincker F, Kervella Y, Zagorska M, DeBettignies R, Peigney A, Flahaut E, Louarn G, Lefrant S, Demadrille R, Pron A. Composites of double-walled carbon nanotubes with bis-quaterthiophene-fluorenone conjugated oligomer: spectroelectrochemical and photovoltaic properties. *Journal of Physical Chemistry C* 2009; **113**:17347–17354.